



A FINE-TUNING WORKFLOW FOR AUTOMATIC FIRST-BREAK PICKING WITH DEEP LEARNING

FINE-TUNING WORKFLOW FOR AUTOMATIC FIRST-BREAK PICKING

 **Amir Mardan***
Geostack
Polytechnique Montréal
QC, Canada
mardan.amir.h@gmail.com

Martin Blouin
Geostack
Québec, QC, Canada
mblouin@geostack.ca

 **Gabriel Fabien-Ouellet**
Polytechnique Montréal
Montréal, QC, Canada
gabriel.fabien-ouellet@polymtl.ca

 **Bernard Giroux**
INRS-ETE
Québec, QC, Canada
bernard.giroux@inrs.ca

Christophe Vergniault
Électricité de France
France
christophe.vergniault@edf.fr

Jeremy Gendreau
Polytechnique Montréal
Montréal, QC, Canada
jeremy.gendreau@polymtl.ca

April 12, 2024

ABSTRACT

First-break picking is an essential step in seismic data processing. For reliable results, first arrivals should be picked by an expert. This is a time-consuming procedure and subjective to a certain degree, leading to different results for different operators. In this study, we have used a U-Net architecture with residual blocks to perform automatic first-break picking based on deep learning. Focusing on the effects of weight initialization on first-break picking, we conduct this research by using the weights of a pretrained network that is used for object detection on the ImageNet dataset. The efficiency of the proposed method is tested on two real datasets. For both datasets, we pick manually the first breaks for less than 10% of the seismic shots. The pretrained network is fine-tuned on the picked shots and the rest of the shots are automatically picked by the neural network. It is shown that this strategy allows to reduce the size of the training set, requiring fine tuning with only a few picked shots per survey. Using random weights and more training epochs can lead to a lower training loss, but such a strategy leads to overfitting as the test error is higher than the one of the pretrained network. We also assess the possibility of using a general dataset by training a network with data from three different projects that are acquired with different equipment and at different locations. This study shows that if the general dataset is created carefully it can lead to more accurate first-break picking, otherwise the general dataset can decrease the accuracy. Focusing on near-surface geophysics, we perform traveltime tomography and compare the inverted velocity models based on different first-break picking methodologies. The results of the inversion show that the first breaks obtained by the pretrained network lead to a velocity model that is closer to the one obtained from the inversion of expert-picked first breaks.

Keywords First-break picking, Near-surface seismic, Deep learning, Segmentation, Transfer learning

Introduction

In a seismic shot record, the first arrival is usually the direct wave from the source followed by refractions at the base of the weathering layer. The first break (FB) is the time taken by a seismic wave to travel from a source to a geophone. First breaks are picked to estimate static corrections (Coppens, 1985; Marsden, 1993), near-surface velocity

*Corresponding author, mardan.amir.h@gmail.com

estimation (Azwin et al., 2013; Fabien-Ouellet and Fortier, 2014), muting parameters for processing reflected data, and microseismic event location (Dip et al., 2021; Nasr et al., 2022). In marine studies, first breaks can be studied to also estimate the location of hydrophones (Walia and Hannay, 1999) as well as modeling the water velocity variation, which is highly important for time-lapse seismic studies (Mardan et al., 2023).

First breaks are conventionally picked manually. Manual picking is a labor-intensive and time-consuming processing step which can take up to 30% of the processing time (Sabbione and Velis, 2010). This is also a subjective task that leads to different results for different operators. To mitigate this problem, numerous methods have been introduced with the aim of automating the process. Zwartjes and Yoo (2022) classified these methods into three classes; cross-correlation based, energy-based, and neural-network (NN) based. Peraldi and Clement (1972) proposed a method to automate the first-break picking based on the cross-correlation of adjacent traces in a seismic shot. Finding the maximum cross-correlation between traces, they can estimate the time delay between first breaks in different traces. This method has difficulty to detect first breaks efficiently in a seismic shot with bad or dead traces (Figure 1a). Coppens (1985) proposed a method to automate first-break picking based on the energy ratio of the signal in two windows with different sizes. This method is called short-term-average over long-term average (STA-LTA) and its efficiency decreases in noisy data (Figure 1b). Although other methods such as modified Coppens' method (Sabbione and Velis, 2010), entropy method (Sabbione and Velis, 2010), and statistical methods (Hatherly, 1982) have been proposed to improve the accuracy of automatic first-break picking, these methods usually require an expert to select parameters such as window length and threshold among others, which increases human bias in this processing step.

Nowadays, numerous seismic data acquisitions are carried out every day around the globe using efficient techniques such as distributed-acoustic sensing (DAS) or landstreamers, with the consequence that the volume of seismic data that must be processed is significantly increasing. In this regard, artificial intelligence (AI) has been used to improve the seismic data processing and interpretation workflow (Zhao and Mendel, 1988; Veezhinathan and Wagner, 1990; Röth and Tarantola, 1994; Lim, 2005; Leite and Vidal, 2011; Mardan et al., 2017; Fabien-Ouellet and Sarkar, 2020; Alali et al., 2022; Mardan and Fabien-Ouellet, 2024). With the focus on automatic first-break picking, researchers started employing NN in the early 1990s (Veezhinathan and Wagner, 1990; Murat and Rudman, 1992; McCormack et al., 1993). With subsequent development in computational power and NN techniques, convolutional neural network (CNN) has been employed to improve the accuracy of automatic picking by taking the spatial coherency of data into account. Yuan et al. (2018) employed a CNN to classify the data on a seismic shot into two groups: FB and non-FB. They showed the potential of CNN for first-break picking. However, preparing the training data for this strategy is challenging and time consuming (if not more than manual first-break picking). To mitigate this problem, first-break picking has been considered as a semantic segmentation problem. Hu et al. (2019) employed a U-Net (Ronneberger et al., 2015) architecture to train a network for first-break picking based on segmenting a seismic section into FB and non-FB. They widened the FB segment to three pixels around picked first-break to increase the accuracy. Their workflow does not require picking non-FB for data preparation. Nevertheless, it suffers from data imbalance which is a common challenge for image segmentation (Hossain et al., 2021).

As is shown in Figure 1c, a seismic shot can be segmented into before and after FB. In this way, FB can be automatically picked as the interface between two segments. Considering first-break picking as a segmentation problem, Wu et al. (2019) and Yuan et al. (2022) employed SegNet (Badrinarayanan et al., 2017) to automate the procedure. Wu et al. (2019) trained SegNet on traces of microseismic sections to predict first-arrivals. They assessed the efficiency of SegNet for detecting first arrivals in synthetic data with different signal-to-noise ratio (SNR) and in field data. They showed the superiority of CNN-based method over STA-LTA method. Yuan et al. (2022) employed a SegNet architecture to autopick first breaks on real seismic shots with sparsely distributed traces. They showed that the CNN-based methods can give good performance for processing sparse data.

U-Net is another network architecture that has been used to pick first breaks accurately by performing segmentation. Zhu and Beroza (2019) introduced PhaseNet by modifying U-Net to process 1D time-series data. For an accurate first-arrival picking of P - and S -waves, they picked the first arrivals manually in 700,920 traces that were used in the training process. Focusing on earthquake data, Zhu and Beroza (2019) showed that the trained PhaseNet was able to provide higher accuracy than STA-LTA. Ma et al. (2020) used a U-Net to automate first-break picking in microseismic and borehole studies. They investigated the effects of noise level in data and shape of the input data (1D or 2D seismic data) on the performance of the network. Zwartjes and Yoo (2022) compared different architectures and training parameters aiming to find crucial parameters in CNN-based automatic first-break picking. Comparing auto-encoder, U-Net, and U-Net with residual blocks, Zwartjes and Yoo (2022) showed that standard U-Net is computationally less demanding, while U-Net with residual blocks can lead to a better generalization and requires fewer epochs to reach a specific loss.

The aforementioned methods have different degree of accuracy in the presence of noise. Effects of noise on results are more pronounced when receivers record strong noise before the arrival of direct and refracted waves (Figure 1c).

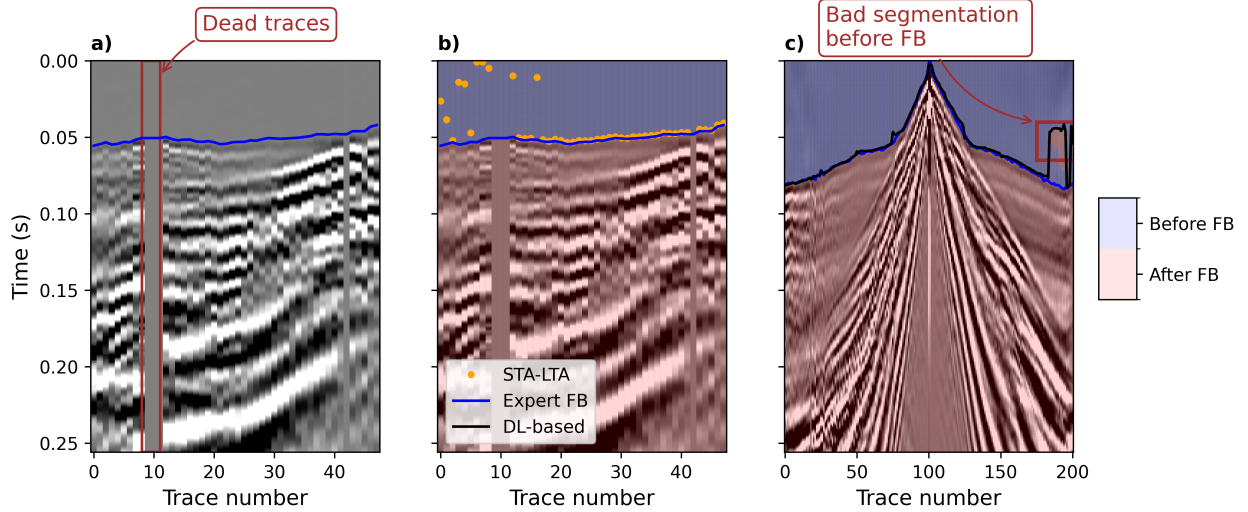


Figure 1: An example of automatic first-break picking, its challenges, and seismic shot segmentation. (a) An example of seismic shot with corresponding FB picked by an expert (blue line). Red rectangle shows some dead traces whose corresponding geophones have not been active during the acquisition. (b) A shot gather with first breaks picked by an expert and STA-LTA method (orange dot). (c) In data segmentation a shot gather is divided into two segments as before FB (blue) and after FB (red) whose interface is the predicted FB as shown with black line. Bad segmentation is shown with red rectangle.

Although DL has shown the highest accuracy to automate the first-break picking compared to cross-correlation and energy-based methods, it can be seen in the mentioned studies that the presence of noise before FBs remains challenging. Performance of DL-based methods also relies drastically on the size of the dataset. The motivation of this study is to increase the accuracy of automatic first-break picking while decreasing the required size of the training dataset. This makes the DL-based FB picking applicable to near surface surveys, because training from scratch and building a training set with usual strategy is presently too costly for near surface studies. To achieve this goal, we employ transfer learning (Bozinovski and Fulgosi, 1976; Goodfellow et al., 2016). Transfer learning is a machine learning technique where the knowledge that a model has obtained to perform a task can be used to improve the learning of a new task (Goodfellow et al., 2016). This technique has shown its potential to mitigate the challenges of using AI in geophysical problems (Cunha et al., 2020; Park and Sacchi, 2020; Simon et al., 2023). In these studies, authors first train a network on a simple or synthetic dataset and then fine tune the parameters of the network with more complex or field data.

All previous studies on DL-based first-break picking use random initialization. In this work, we investigate if the knowledge that a network has obtained from solving a non-geoscientific problem can be helpful for solving first-break picking. In this regard, we design an architecture based on U-Net (Ronneberger et al., 2015) with residual blocks (He et al., 2016) as its encoder, to perform automatic first-break picking. We show how the weights used for solving the ImageNet challenge (Deng et al., 2009) can increase the segmentation accuracy and lead to a more accurate first-break picking and reduce the size of the required training set to attain a fixed accuracy. The small size of the required dataset for training allows to fine tune the network on a per survey basis which makes our method applicable to most near surface surveys. We propose a workflow in which a small fraction (around 10%) of the survey is picked by a human expert, then the NN is fine tuned and picks automatically the rest of the survey. In the current study, we analyze this strategy by applying the methodology to two refraction surveys used for near surface investigation.

This paper is organized as follows. First, we present the methodology including data preparation, architecture of the neural network, and loss function. Next, we study the efficiency of the proposed method to pick FBs using two different datasets (with high and low SNR). We then show how creating a general dataset can affect first-break picking by comparing the accuracy after training using a project-based dataset and using a general dataset. At the end, we assess the quality of the automatically picked first breaks by comparing velocity models obtained with travel time tomography.

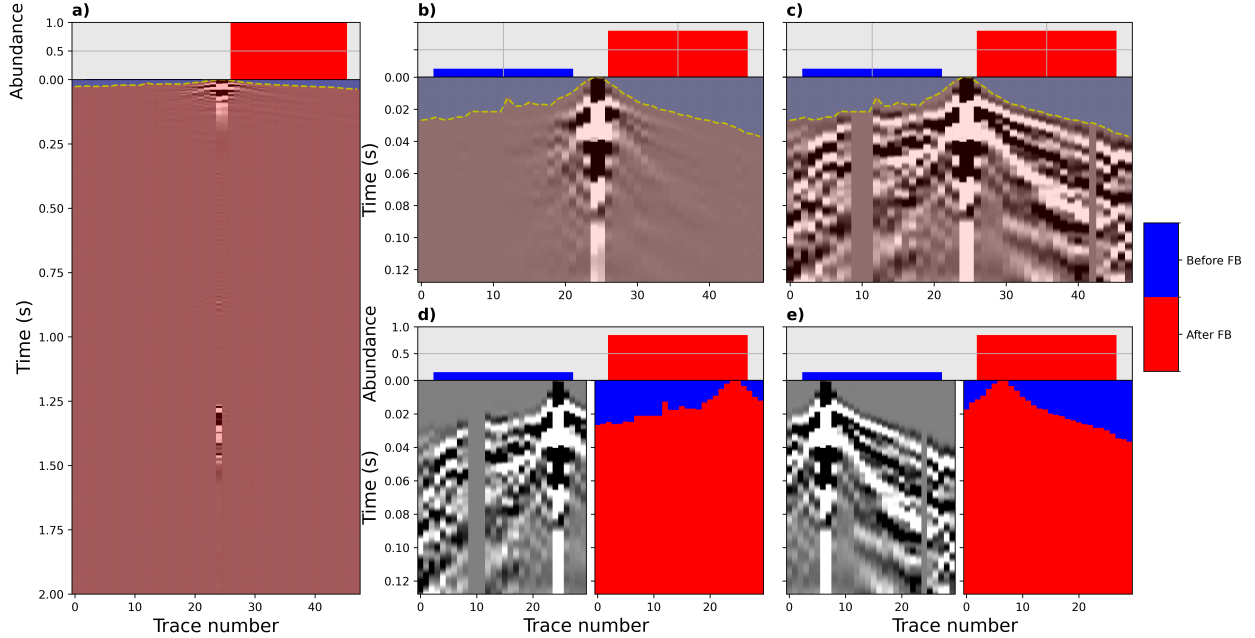


Figure 2: The data preparation strategy employed for this study. (a) A raw seismic shot is (b) cropped, (c) scaled, and (d-e) divided to subimages. The relative abundance of data in each segment is shown as bar plots above each seismic shot where blue indicates before FB and red demonstrates after FB. Yellow line shows the manually picked FB.

Methodology

Data preparation

The key to have an efficient network that can predict with high accuracy is training with a suitable dataset. A network should be trained with a large amount of data and the data should represent all possible scenarios that might exist in the real-world problem that is tackled. Considering first-break picking as a segmentation problem, we need pairs of seismic shots and their corresponding FBs to train the network.

A common challenge in segmentation is class imbalance which reduces the accuracy of the network to predict the right segment for the minority-segment region (Hossain et al., 2021). Class imbalance means that the number of pixels in one segment is significantly higher than the number of pixels in other segments. Figure 2a shows a raw seismic shot (bottom) that is used in this study for training the network. The relative abundance of data from each segment is shown in the top part of Figure 2a. As can be seen, almost all data samples belong to after FB (99.0%). Due to the fact that we are only interested in finding the first breaks, we can crop the seismic shot to improve the balance between segments (Figure 2b). This reduces the relative abundance of after FB to 84.7%.

In the next step, we scale each trace by its maximum amplitude (Figure 2c) to facilitate learning in the training phase. In the final step and based on number of traces in each seismic shot, shot gathers are divided into smaller sections with a specific overlap (Figure 2d and 2e). This data augmentation process can improve accuracy of the network by diversifying the training data. At the end of processing, pairs of image-label are obtained from a raw seismic shot (Figure 2a) as shown in Figure 2d and 2e.

Network architecture

The neural network employed in this study is based on U-Net (Ronneberger et al., 2015) as presented in Figure 3. U-Net is a fully convolutional encoder-decoder network with long skip-connections between encoder and decoder that helps to have a smoother loss leading to faster training (Li et al., 2018). The input of the network is a one-channel patch of upsampled subimages $x \in \mathbb{R}^{512 \times 256 \times 1}$. This input size allows to have the desired depth for the employed network. Through the network, we successively downsample the spatial resolution of the input to catch the higher-level features. We use residual blocks (He et al., 2016) to build the encoder which can help to prevent the gradient vanishing problem (Zwartjes and Yoo, 2022).

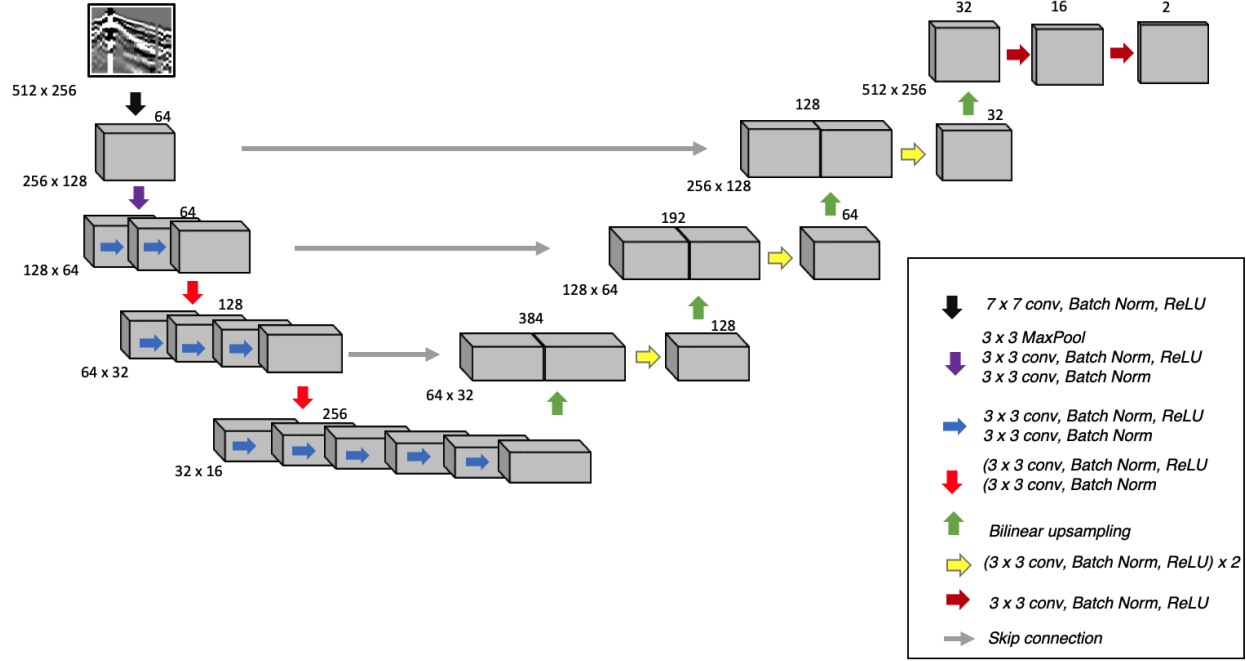


Figure 3: U-Net architecture with ResNet encoder where the purple, blue, and light red arrows in the encoder show the residual blocks.

At the lowest level of the network, the output of the encoder is a patch of $x \in \mathbb{R}^{32 \times 16 \times 256}$. The decoder acts as an expanding path which builds a segmentation map from the encoded features. The decoder includes four blocks. Each block duplicates the spatial resolution by performing a bilinear upsampling. Using skip connection, the result of upsampling is concatenated with the output of its symmetric block in the encoder. At each step, the concatenated tensor is passed into two convolution operators in addition to batch normalization and rectified linear unit (ReLU) operators to halve the number of channels with respect to the output of the previous decoding block. At the end, the output of the network is a probability image $P(x) \in [0, 1]^{512 \times 256 \times 2}$ which contains two channels corresponding to the predicted probability of each class (before FB and after FB).

Loss function and optimization

In this study, the cross-entropy loss function is used to measure the accuracy of the segmentation. This loss function for one sample (subimage) can be written as

$$E = - \sum_i y_i \log(\hat{y}_i), \tag{1}$$

where y_i and \hat{y}_i are the given and predicted segments for pixel $i \in \Omega$ with $\Omega \subset \mathcal{Z}^2$.

The output of the network is the probability of each pixel to fall in one of the two segments. The final segmentation can be obtained by passing this probability tensor into an argmax operator which can be defined as equation 2 for function f ,

$$\operatorname{argmax} f := \{x : f(s) \leq f(x) \text{ for all } s \in X\}. \tag{2}$$

Equation 2 allows to build the segmentation map, $\Phi(x) \in [0, 1]^{512 \times 256 \times 1}$, from the probability image, $P(x)$.

The cross-entropy loss function (equation 1) can be used to perform an accurate segmentation for first-break picking (Wu et al., 2019; Zhu and Beroza, 2019; Ma et al., 2020; Zwartjes and Yoo, 2022). While equation 1 is used to train and evaluate the network for segmentation, we also used the root-mean-squared error (RMSE) to measure the error for predicting the FBs in a dataset as,

$$\operatorname{RMSE} = \sqrt{\frac{\sum_{i=1}^N (x_i - \hat{x}_i)^2}{N}}, \tag{3}$$

where x_i and \hat{x}_i are the given and predicted FB for trace i in a shot with N traces. It should be mentioned that equation 3 is not involved in training and it is only employed to measure the accuracy of the network for first-break picking.

Employing the Adam optimization method (Kingma and Ba, 2014), the network parameters are optimized to reduce the loss based on equation 1. In all case studies, we use a learning rate of 1×10^{-4} and each batch of training data includes 15 pairs of subimages and their corresponding labels.

Parameter initialization

To train a network, loss is decreased through an iterative method. Thereby, initial weights are required to start the training and the performance of most algorithms are affected by the initial weights of the network (Goodfellow et al., 2016). Even with a very large training dataset, the effects of an efficient initialization are considerable (Glorot and Bengio, 2010) and an ineffective initialization can prevent the training to converge (Goodfellow et al., 2016). Besides, preparing a large and comprehensive dataset for training is expensive and time-consuming. Transfer learning is a technique that allows us to mitigate these problems. Using this technique, we can transfer the knowledge that a network has learned in one setting to improve generalization in another setting (Goodfellow et al., 2016). Thereby, a network can be initialized using pretrained weights of another network and fine-tuned to pick FBs accurately.

In this study, we assess the effects of two different initializations strategies to improve the accuracy of automatic first-break picking. In addition to random initialization, we use the weights of a pretrained resnet-34 to initialize the encoder presented in Figure 3. The pretrained resnet-34 is trained to solve the ImageNet classification problem (Deng et al., 2009). The ImageNet is a database of more than 14 million images and in the next section, we assess the effects of initializing the encoder using the parameters of the pretrained resnet-34. For this purpose, we have performed three tests and have trained three networks for each test:

- training using ImageNet weights with 20 epochs (ImageNet-20),
- training using random initialization with 20 epochs (Random-20),
- training using random initialization with 100 epochs (Random-100).

All networks are trained using Adam optimization with a learning rate of 1×10^{-4} .

Results

In this study, we use datasets from three different land surveys to perform three experiments (named Experiment 1 - 3). Dataset characteristics of each experiment are presented in Table 1. There are 244 and 291 seismic shots in Dataset 1 and Dataset 2, respectively. Seismic source in Dataset 1 is an Isotta energizer while seismic data in Dataset 2 are obtained using a sledge hammer.

In Experiment 1, we use 21 seismic shots from Dataset 1 (less than 9% of the shots) to train and evaluate the networks. Then, the trained networks are used to perform the first-break picking on the remaining 223 seismic shots. This experiment is conducted to study the efficiency of different initialization strategies for analyzing clean seismic data (Dataset 1).

Name	Total number of shots	Number of shots for training and testing	Number of traces per shot	Number of subimages per shot	Number of subimages for training
Dataset 1	244	21	101 to 201	4 to 8	133
Dataset 2	291	20	48	3	54
Dataset 3 (general)	585	91	48 to 201	2 to 8	277

Table 1: The used datasets in this study and their characteristics.

The seismic data in Dataset 1 were acquired in the eastern bank of the Rhône river in France (Figure 4a). The profile (yellow line) has a South-East to North-West direction, on the top of Cuijanet syncline crossing the Marsanne fault (black line). In the northwestern part, the Barremian limestone is almost outcropping. In its southeastern part, the fluvial alluvium covers the Albian and Cenomanian conglomerates, themselves covering Albian sandstone. For this acquisition, the seismic sources were placed on the profile with a spacing of 2 m.

In Experiment 2, we analyze the network for performing first-break picking on noisy data (Dataset 2). Only 20 seismic shots out of 291 ($\sim 7\%$) are labeled manually and used to train the network in this experiment. Dataset 2 is highly noisy and first-break picking is very challenging even for a human operator.



Figure 4: Acquisition lines for the data studied in (a) Experiment 1 and (b) Experiment 2. Yellow lines show the acquisition profiles and black line shows the Marsanne fault in the study area. White circle denotes an exploration well in the study area.

This dataset is from a near-surface seismic survey acquired with a 48-channel system in Saint-Liboire in Quebec, Canada (Figure 4b). In this study, the spacing between seismic sources is 2.5 m and the receivers are placed at every 5 m. In this project, seismic refraction tomography was used in combination with electrical resistivity tomography for characterizing the aquifer with the ultimate goal of finding an appropriate location for a water well. To increase the SNR, seismic shots in Dataset 2 are a stack of 3 to 5 recordings at each location. Nevertheless, these data have a poor SNR. Hence, this dataset is a good candidate to analyze the efficiency of the proposed automatic FB picking method with noisy data.

After studying the efficiency of different initialization strategies for picking FBs on clean and noisy seismic data, we focus on creating a general dataset (Dataset 3) through Experiment 3. This can help us to understand the efficiency of the DL-based first-break picking if we augment the training dataset by combining the data obtained under different circumstances (i.e. various equipment, acquisition parameters, and geology of the study areas). Dataset 3 is built by combining Dataset 1, Dataset 2, and 50 seismic shots (with picked FB) from a third project where sledge hammer is used as seismic source. The data in these three datasets are acquired by different companies and different equipment at different locations. It is better to have a single specialist to prepare the training dataset to reduce the subjectivity of the results. However, the first breaks in Dataset 3 were picked by three different experts in the present case. Although this is not ideal, it affects all three networks equally and it should not impact the results of this study, because we compare all the employed networks under the same circumstances and data preparation is the same for all these networks.

As presented in Figure 2 and Table 1, the seismic shots are converted to the different numbers of subimages (based on the number of available traces) for each project. For each experiment, we use 90% of the labeled data to train the network and the other 10% as a testing set.

Data with high signal-to-noise ratio (Experiment 1)

For Experiment 1, a dataset with good SNR (Dataset 1) has been used. The training dataset for this project includes 21 seismic shots with variable number of traces per shot. These seismic shots are divided into subimages of 30 traces with 15% overlap. Figure 5a-5c shows three examples of seismic shots that have been used to train the network. The manually picked FBs (solid blue line) are presented in addition to the FBs picked using DL and STA-LTA. As is shown, with the same number of epochs, the network that is initialized using ImageNet (dashed red line) is more accurate than the network that is initialized using random weights (dotted purple line). The final training losses for Random-100, Random-20, and ImageNet-20 are presented in Table 2. Using 100 epochs, the network with random initialization leads to the same accuracy as ImageNet-20 for segmentation of the training dataset. However, more epochs causes overfitting as the test loss of Random-100 is higher than that of ImageNet-20 (Table 2). In Figure 5, we can also see the effects of noise on the STA-LTA results (orange dots). In traces with larger offset, the efficiency of STA-LTA decreases, so does the efficiency of Random-20 and Random-100.

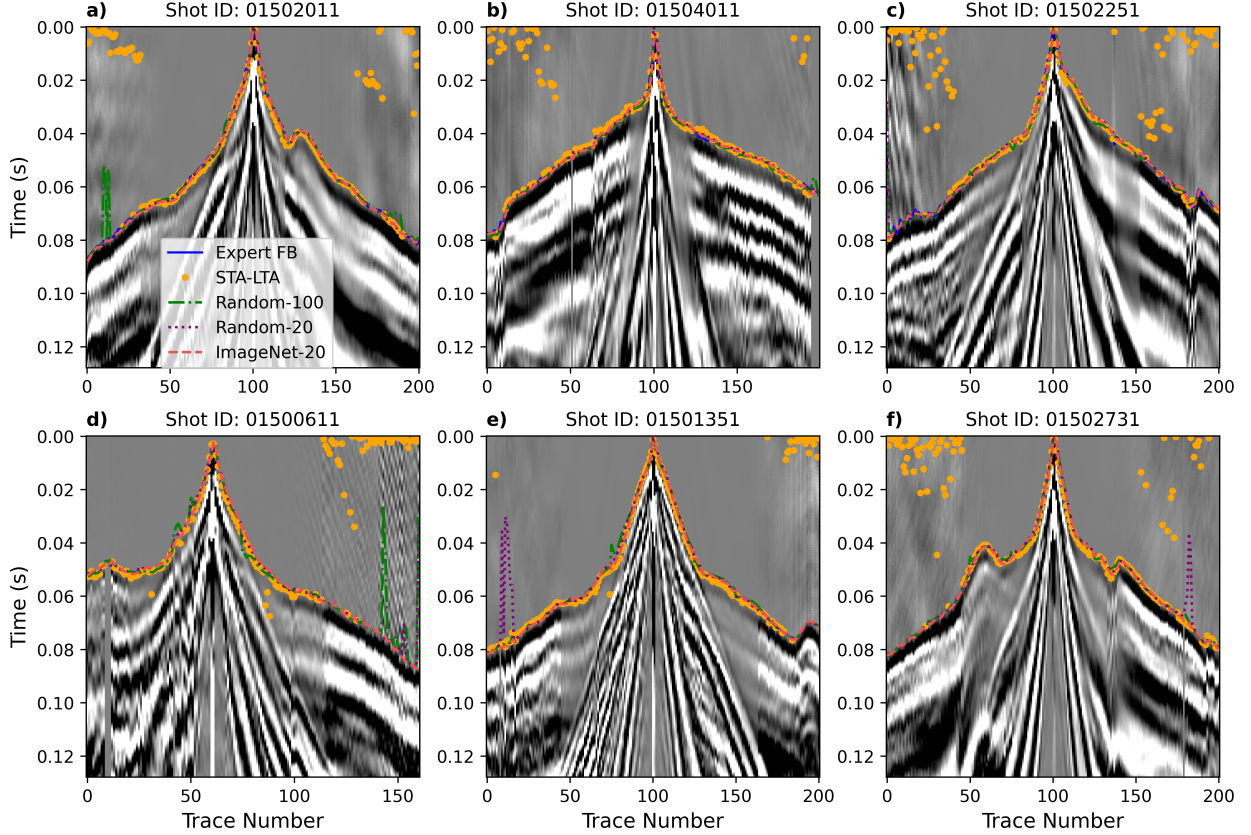


Figure 5: Results of FB picking on (a-c) labeled and (d-f) unlabeled datasets for the data with high SNR. The solid blue line shows the manually picked FB while the results of STA-LTA are shown with orange dots. The dash-dotted green line shows the results using random initialization with 100 epochs. The dotted purple and the dashed red lines show the picked FB using the same number of epochs with different initialization (random and ImageNet respectively).

	Experiment 1 (High SNR)			Experiment 2 (Low SNR)			Experiment 3 (General data)		
	Training	Test	FB RMSE	Training	Test	FB RMSE	Training	Test	FB RMSE
ImageNet-20	0.026	0.039	0.425	0.073	0.126	0.941	0.018	0.030	0.394
Random-20	0.029	0.072	0.614	0.070	0.156	0.990	0.020	0.051	1.0
Random-100	0.026	0.067	1.0	0.068	0.159	1.0	0.017	0.052	0.969

Table 2: The segmentation loss and normalized first-break picking loss for different tests and networks.

In the next step, the trained networks are employed to detect the FBs in the unlabeled data. The results are shown in Figure 5d-5f. As for the test set, these shot gathers have not been seen before by the networks. However, in this case, no first breaks were manually picked. Initializing the network using ImageNet leads to the most accurate result, while increasing number of epochs for training randomly initialized networks does not improve the results significantly (Table 2).

To train the networks, the cross-entropy loss function (equation 1) is used to evaluate the accuracy of the results, numerically. Although the loss value shows the accuracy of each network for segmentation, this parameter is not really representative for first-break picking quality. This is due to the fact that bad segmentation of even one pixel before the FB, can lead to erroneous picked FB (Figure 1c). On the other hand, bad-segmentation after the FB, does not affect the accuracy of picked FB while it still affects the value of the segmentation loss. The final accuracy of segmentation and the normalized first-break picking errors (equation 3) for Random-100, Random-20, and ImageNet-20 are presented in Table 2. This experiment shows that initializing a network with weights of a pretrained network leads to more accurate first-break picking for seismic data with high SNR.

Data with low signal-to-noise ratio (Experiment 2)

For the second experiment, we focus on picking FBs in seismic data with low SNR (Dataset 2). We have picked the FBs on 20 seismic shots (out of 291) used 18 as training data and 2 as test data. We divided each shot into three subimages. Each subimage is created using 22 traces from the corresponding seismic shot with 15% overlap with other subimages.

Figure 6a-6c shows the results of automatic first-break picking for three examples from the training dataset. While the performance of all three networks is comparable in most seismic shots, random initialization of the network with 100 epochs leads to higher training accuracy. Results of STA-LTA for this dataset show that this method is completely unreliable to pick the FBs on such a noisy dataset.

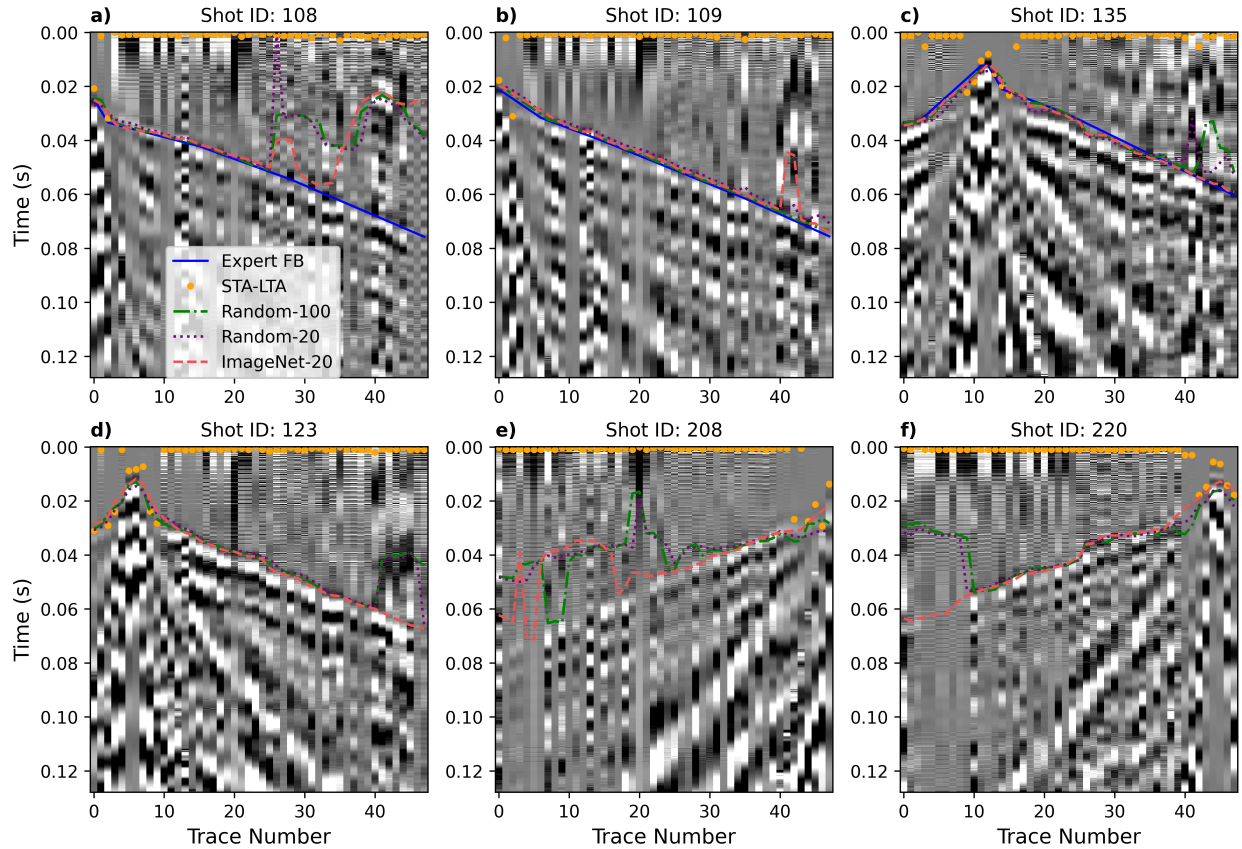


Figure 6: Results of FB picking on (a-c) labeled and (d-f) unlabeled datasets for the data with low SNR. The solid blue line shows the manually picked FB while the results of STA-LTA are shown with orange dots. The dash-dotted green line shows the results using random initialization with 100 epochs. The dotted purple and the dashed red lines show the picked FB using the same number of epochs with different initialization (random and ImageNet respectively).

The training and test losses for Experiment 2 are presented in Table 2. The final training losses for Random-100, Random-20, and ImageNet-20 are respectively 0.068, 0.070, and 0.073. While Random-100 provides the highest training accuracy, the goal is to train a network that can have the highest test accuracy. This is the case for ImageNet-20 where the network is pre-trained. Based on the test loss, ImageNet-20 is more powerful for performing the segmentation of test dataset, with a loss of 0.126 in comparison to Random-20 and Random-100 with losses of 0.156 and 0.159. The first-break picking errors for the networks also demonstrates higher accuracy of ImageNet-20.

Applying the trained networks on the unlabeled data, we can again see the advantage of using ImageNet-20 over Random-20 and Random-100. Using pretrained weights, the network is better at picking FBs. Nevertheless, these data are highly noisy and even the ImageNet-20 has problem in some seismic shots (e.g. Figure 6a in training set and Figure 6e from unlabeled dataset). It should be pointed out that picking the right FBs in these seismic shots can be also a very challenging task for an expert. For data with this level of noise, supervision of an expert is unavoidable. However, for

the sake of making a comparison between the studied networks, we can see that ImageNet-20 is more accurate for first-break picking and segmenting the test dataset.

General dataset (Experiment 3)

For the third experiment, we mixed the labeled datasets of the first two case studies with another 50 seismic shots that have acquisition geometry similar to the seismic shots in Dataset 2. As shown in Table 1, Dataset 3 includes 244 seismic shots from Dataset 1 and 291 seismic shots from Dataset 2. The 50 seismic shots from the other study have 48 traces, and 30 traces are used to create the corresponding subimages. This allows us to add 100 examples to the training and test datasets. In total, the labeled dataset for this experiment includes 308 shots from which 90% are used as training set (277 subimages) and 10% as test set (31 subimages).

The segmentation and FB picking losses for the three networks are presented in Table 2. The test loss shows the better generalizability of ImageNet-20 with loss of 0.030 in comparison with 0.051 and 0.052 for Random-20 and Random-100. The first-break picking error of this experiment also shows the superiority of the ImageNet-20.

The results of applying the trained networks on four examples are shown in Figure 7. Figure 7a and 7b belong to the training dataset while Figure 7c and 7d are part of the unlabeled dataset. Comparing Figure 7a with Figure 5c shows that the strategy of adding training data from different projects cannot guarantee better accuracy. This is shown in Table 3 where project-based training dataset led to higher accuracy for Dataset 1 in comparison to using the general dataset. On the contrary, Table 3 shows that the general dataset increased the accuracy for first-break picking of shots in Dataset 2 (comparing Figure 7b with Figure 6a). This can be due to the fact that in addition to 20 seismic shots that are common between Dataset 2 and Dataset 3, another 50 shots have similar seismic source and acquisition geometry to Dataset 2 (Table 1). It means 78% of the shots in Dataset 3 have similar acquisition geometry and seismic source. Thereby, training a network using this general dataset leads to higher accuracy for seismic shots in Dataset 2 while less accuracy for seismic shots in Dataset 1.

	Shots from Dataset 1		Shots from Dataset 2	
	Project-based Dataset	General Dataset	Project-based Dataset	General Dataset
ImageNet-20	0.0011	0.0014	0.0014	0.0002
Random-20	0.0016	0.0030	0.0015	0.0013
Random-100	0.0026	0.0029	0.0015	0.0013

Table 3: The first-break prediction loss based on equation 3 for comparing the accuracy of results in case of using project-based or general datasets.

Figures 7c and 7d show two seismic shots from Dataset 1 and Dataset 2, respectively. The FBs are picked using the networks that are trained with general dataset. The results can be compared with Figures 5d and 6e, respectively where project-based datasets are employed to train the networks.

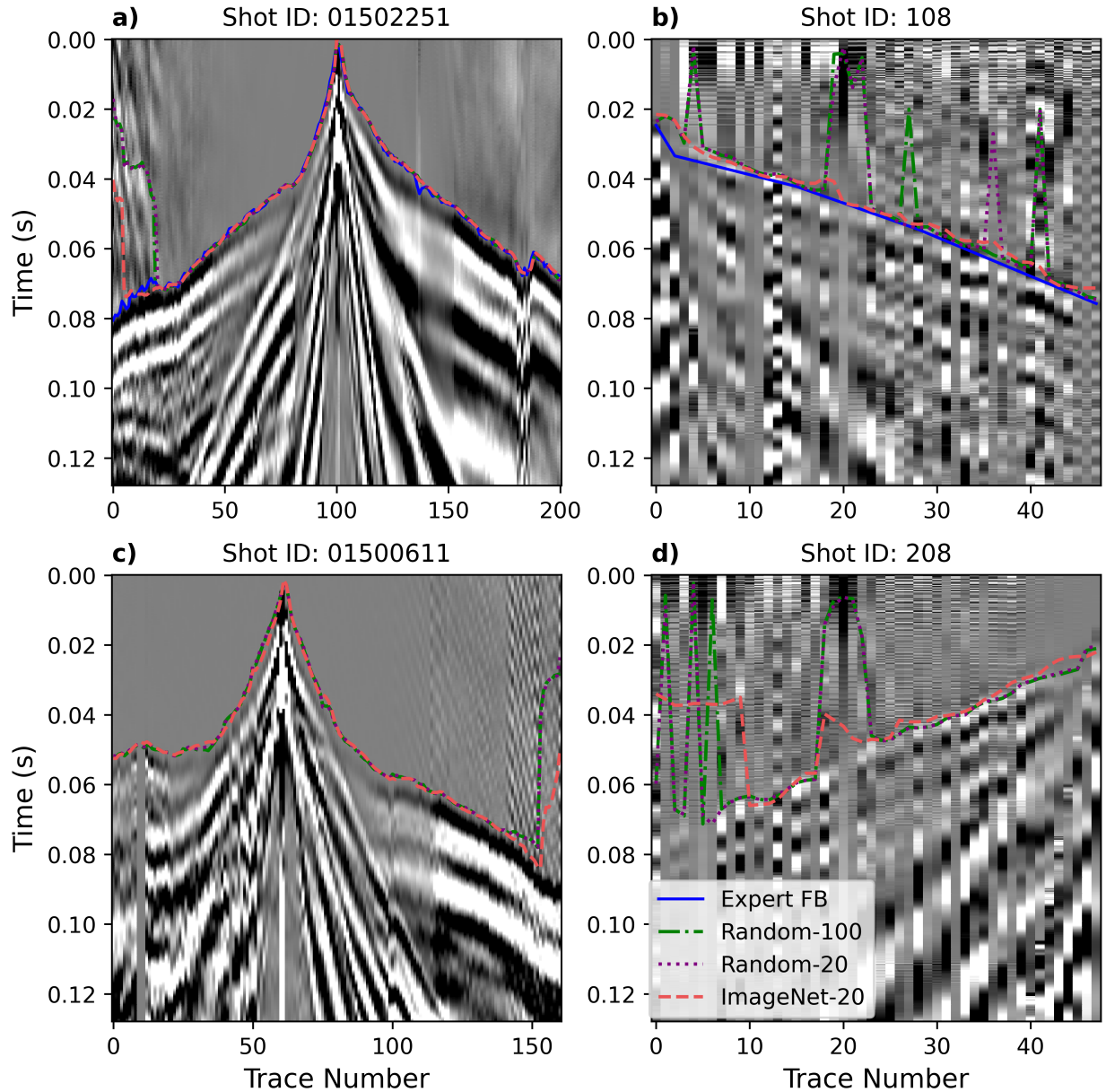


Figure 7: Results for training the network on data from different projects. The solid blue line shows the manually picked FB while the dotted purple and the dashed red lines show the picked FB using the same network with different initialization (random and ImageNet respectively). The dash-dotted green line shows the result of using random initialization with 100 epochs. These examples are (a and b) training (c and d) unlabeled samples of (a and c) Dataset 1 and (b and d) Dataset 2.

Refraction traveltimes tomography

In near surface studies, FBs are usually used to estimate a P -wave velocity (V_P) model of the subsurface. In this section, we inverted the picked FBs of Experiment 1 and Experiment 2 to compare the estimated velocities. This inversion is done using PyGIMLi (Rücker et al., 2017) and based on the shortest path algorithm (Moser, 1991). It allows us to analyze the accuracy of picked FBs in terms of the final outcome of a near surface seismic survey: a P -wave velocity model. Our assessment criterion is that the inversion result of the output of an efficient automatic FB picking method should have the minimum discrepancy with the inversion result obtained from manually picked FBs.

Estimates are shown in Figure 8. The first column shows the results for Experiment 1 and the second column presents the results obtained from Experiment 2. Figure 8a - 8h denotes the estimated velocity from the picks in the labeled dataset (training and test set). V_P estimated from manually picked FBs are shown in Figure 8a and 8b. As indicated by normalized root-mean-squared error (NRMSE) of velocity, the estimates obtained from FBs picked by ImageNet-20 (Figure 8c - 8d) have smaller discrepancy with the ones obtained from manually picked FBs in comparison to estimates from Random-20 (Figure 8e - 8f) and Random-100 (Figure 8g - 8h). Employing Random-20 and Random-100 to detect FBs in Experiment 1 leads to some non-geological structures in the velocity model that are due to inaccurate picks. These anomalies are shown with red arrows.

Based on our workflow, the trained network is used to obtain FBs in all seismic shots. We then verify the obtained FBs and modify them in case of inaccuracy. Using more information and better ray path coverage decrease the uncertainty in traveltimes inversion and leads to higher accuracy. Hence, as ImageNet-20 has provided the most accurate FBs (Table 2), we have used this network to predict the FBs in all seismic shots in Dataset 1 and Dataset 2. These FBs are then verified and inverted to obtain velocity models. The velocity models are shown in Figure 8i and 8j. These models show meaningful images of the subsurface. While Figure 8i does not have anomalies such as the ones denoted with red arrows in other estimates of Experiment 1, Figure 8j shows using more FBs can improve the accuracy of estimate. Picking more FB in Experiment 2 led to a better model of the deeper part of our study area. This can also be seen with comparing the 1D estimations close to the well location (red triangle) which is shown in the right side of the second column (Figure 8). The lithology of the well is color coded based of the drilling report and it can be seen that utilizing more FBs allows better constraining the inversion and leads to higher accuracy in the deeper parts.

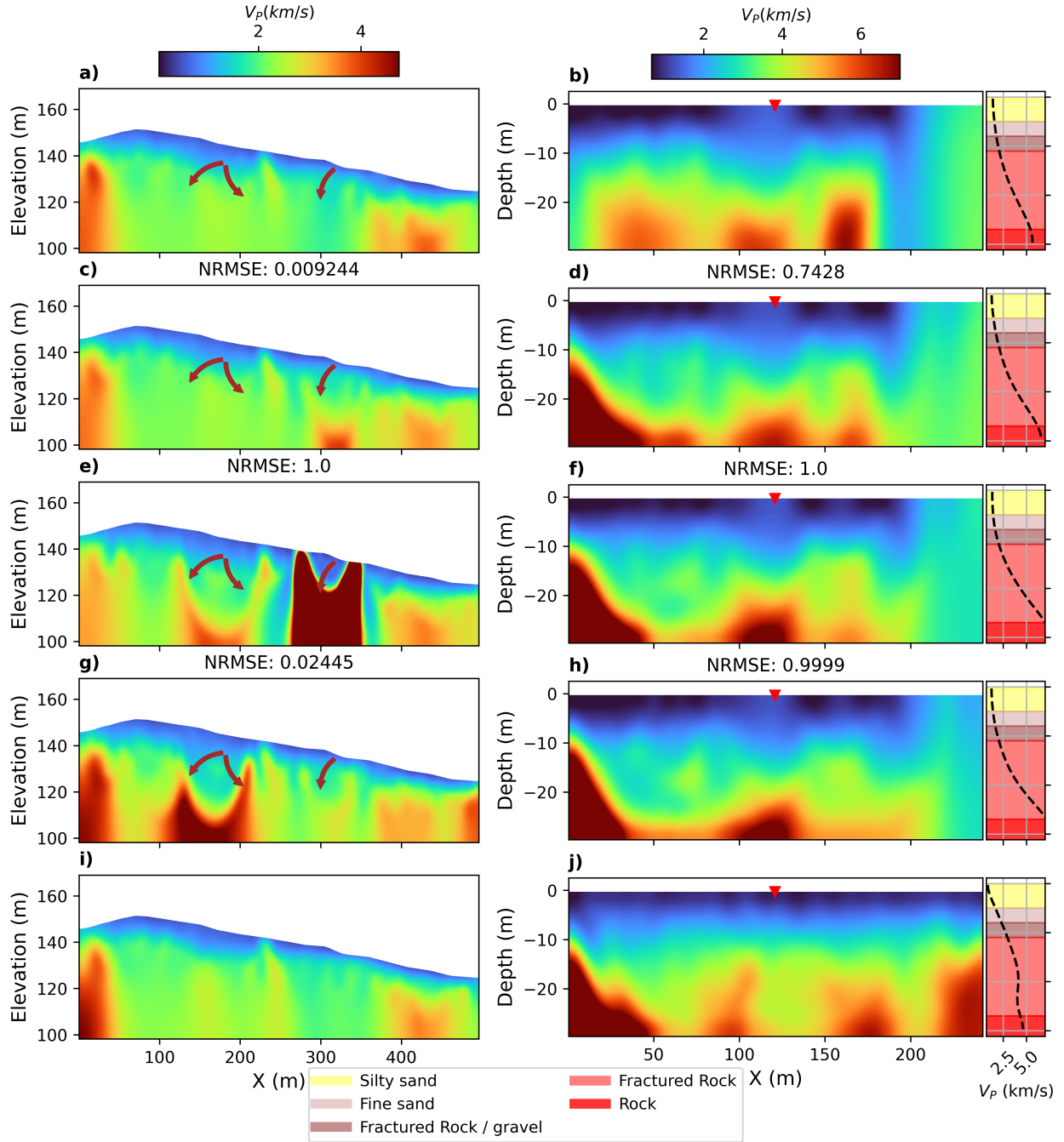


Figure 8: Results of traveltime inversion for Experiment 1 (left column) and Experiment 2 (right column). Results of inversion for first breaks that are involved in training procedure picked by (a and b) an expert, (c and d) ImageNet-20, (e and f) Random-20, and (g and h) Random-100. (i and j) Estimated V_P using FBs of all seismic shots picked by ImageNet-20. Red arrows show the main differences between the estimates from automatically picked FBs and manually-picked ones. Red triangle shows the well location (white circle in Figure 4b). The 1D plots show the estimated velocity at the well location.

Discussion

The effects of weight initialization for DL-based automatic first-break picking is analyzed in this study. Considering a common network and hyperparameters in three different scenarios, it is shown that using pretrained weights can improve the accuracy of picked FBs. To make a fair comparison, the network with random initialization is trained also with more epochs. Considering first-break picking as a segmentation problem, the network with pretrained weights leads to more accurate results for test set while it can lead to a lower training accuracy compared to the randomly initialized networks. This shows that this network is better generalizable. Table 2 presents the segmentation error for the three tests conducted in this study. For these tests, Random-100 provides the lowest training loss while ImageNet-20 provides the highest accuracy for test set. This shows that using random initialization and higher number of epochs can cause overfitting, especially with small training sets as employed in this study. Although the ImageNet challenge is an object recognition problem, the weights of the trained network can be employed in a segmentation problem and lead to a lower test loss than using random values for initializing a network.

As the goal of this study is first-break picking, Table 2 shows the loss between manually picked FBs and predicted FBs using the different networks. As is shown, the ImageNet-20 provides the highest accuracy and the networks with random initialization provide the lowest accuracy.

This study shows that a general training dataset can decrease the accuracy of the network in comparison with project-based training dataset if the dataset is not large enough to represent appropriately different situations such as various types of sources, noise level, geology of the study area (depth of the bedrock), and other acquisition parameters. A better understanding of this fact can allow to create multiple general training datasets for a specific situation (e.g. a general dataset for acquisitions with a sledgehammer as the source or acquisitions with similar geometry).

Besides, it is important to conduct more studies to analyze the effects of data preparation parameters such as the width of subimages and overlap between subimages on the efficiency of DL-based automatic first-break picking. Although this will not affect the fact that initializing the network with pretrained weights leads to more accurate results, it will help one to develop a more effective workflow for automatic first-break picking.

The method we propose is readily applicable on field data. A workflow based on NN fine tuning comprises the following steps:

1. pick the first breaks of a small fraction of shots (between 5 to 10%),
2. prepare the training and testing set as described in the section "data preparation",
3. fine-tune the network on the training set, and monitor overfitting with the test set,
4. apply the fine-tuned network on the remaining shots.

This workflow can lead to a significant reduction in the time required for first-break picking. Indeed, the data preparation can be fully automated and is a rather straightforward task. The network training is also fast and cheap, as the training set can be small using fine-tuning. For instance, training in this study was conducted on a laptop with an Apple M1 Max chip and it took 86.76 seconds and 26.74 seconds for Experiment 1 and Experiment 2, respectively.

Conclusions

An efficient automatic first-break (FB) picking based on artificial intelligence relies significantly on the size of training dataset whose preparation and processing are costly and time consuming. This study focuses on reducing the size of required dataset for training a network while not compromising the accuracy. In this regard, we have proposed performing automatic first-break picking by fine-tuning a neural-network pretrained on ImageNet. A U-Net architecture with residual encoder has been used for this study. Using random initialization, we have shown that the network has lower accuracy than in the case of using pretrained weights (ImageNet challenge in this study). This strategy allows to use only 5 to 10% of seismic data from one project to train a network and perform automatic picking with high accuracy on the remaining shots. We have shown that using first breaks obtained by random initialization can lead to non-geological features in the velocity model estimated using the FBs. Comparing with short-term-average over long-term-average method, we have also shown that the proposed deep learning based autopicking provides more accurate results especially in the presence of noise and in seismic shots with low signal-to-noise ratio. Finally, we have demonstrated that using a general training dataset for various projects might cause a decrease in the accuracy of picked FBs if the dataset is biased toward a specific acquisition geometry.

Acknowledgement

This work was supported by Mitacs through the Mitacs Elevate Program.

Data and code availability statement

Python package for performing first-break picking based on the presented workflow is available at https://github.com/geo-stack/first_break_picking. Data associated with this research are confidential and cannot be released.

Conflict of interest

All authors declare that they have no known financial interests or personal relationships that could have influenced the work presented in this paper.

References

- Alali, A., V. Kazei, M. Kalita, and T. Alkhalifah, 2022, Deep learning unroofing for robust subsalt waveform inversion: Geophysical Prospecting; doi: [10.1111/1365-2478.13193](https://doi.org/10.1111/1365-2478.13193).
- Azwin, I., R. Saad, and M. Nordiana, 2013, Applying the seismic refraction tomography for site characterization: APCBEE procedia, **5**, 227–231; doi: [10.1016/j.apcbee.2013.05.039](https://doi.org/10.1016/j.apcbee.2013.05.039).
- Badrinarayanan, V., A. Kendall, and R. Cipolla, 2017, SegNet: A deep convolutional encoder-decoder architecture for image segmentation: IEEE transactions on pattern analysis and machine intelligence, **39**, 2481–2495; doi: [10.1109/TPAMI.2016.2644615](https://doi.org/10.1109/TPAMI.2016.2644615).
- Bozinovski, S., and A. Fulgosi, 1976, The influence of pattern similarity and transfer learning upon training of a base perceptron B2: Proceedings of Symposium Informatica, 121–126.
- Coppens, F., 1985, First arrival picking on common-offset trace collections for automatic estimation of static corrections: Geophysical Prospecting, **33**, 1212–1231; doi: [10.1111/j.1365-2478.1985.tb01360.x](https://doi.org/10.1111/j.1365-2478.1985.tb01360.x).
- Cunha, A., A. Pochet, H. Lopes, and M. Gattass, 2020, Seismic fault detection in real data using transfer learning from a convolutional neural network pre-trained with synthetic seismic data: Computers & Geosciences, **135**, 104344; doi: [10.1016/j.cageo.2019.104344](https://doi.org/10.1016/j.cageo.2019.104344).
- Deng, J., W. Dong, R. Socher, L.-J. Li, K. Li, and L. Fei-Fei, 2009, ImageNet: A large-scale hierarchical image database: 2009 IEEE conference on computer vision and pattern recognition, IEEE, 248–255.
- Dip, A. C., B. Giroux, and E. Gloaguen, 2021, Microseismic monitoring of rockbursts with the ensemble Kalman filter: Near Surface Geophysics, **19**, 429–445; doi: [10.1002/nsg.12158](https://doi.org/10.1002/nsg.12158).
- Fabien-Ouellet, G., and R. Fortier, 2014, Using all seismic arrivals in shallow seismic investigations: Journal of Applied Geophysics, **103**, 31–42; doi: [10.1016/j.jappgeo.2013.12.009](https://doi.org/10.1016/j.jappgeo.2013.12.009).
- Fabien-Ouellet, G., and R. Sarkar, 2020, Seismic velocity estimation: A deep recurrent neural-network approach: Geophysics, **85**, U21–U29; doi: [10.1190/geo2018-0786.1](https://doi.org/10.1190/geo2018-0786.1).
- Glorot, X., and Y. Bengio, 2010, Understanding the difficulty of training deep feedforward neural networks: Proceedings of the thirteenth international conference on artificial intelligence and statistics, JMLR Workshop and Conference Proceedings, 249–256.
- Goodfellow, I., Y. Bengio, and A. Courville, 2016, Deep learning: MIT press.
- Hatherly, P., 1982, A computer method for determining seismic first arrival times: Geophysics, **47**, 1431–1436; doi: [10.1190/1.1441291](https://doi.org/10.1190/1.1441291).
- He, K., X. Zhang, S. Ren, and J. Sun, 2016, Deep residual learning for image recognition: Proceedings of the IEEE conference on computer vision and pattern recognition, 770–778.
- Hossain, M. S., J. M. Betts, and A. P. Paplinski, 2021, Dual focal loss to address class imbalance in semantic segmentation: Neurocomputing, **462**, 69–87; doi: [10.1016/j.neucom.2021.07.055](https://doi.org/10.1016/j.neucom.2021.07.055).
- Hu, L., X. Zheng, Y. Duan, X. Yan, Y. Hu, and X. Zhang, 2019, First-arrival picking with a U-net convolutional network: Geophysics, **84**, U45–U57; doi: [10.1190/GEO2018-0688.1](https://doi.org/10.1190/GEO2018-0688.1).
- Kingma, D. P., and J. Ba, 2014, Adam: A method for stochastic optimization: arXiv preprint arXiv:1412.6980; doi: [10.48550/arXiv.1412.6980](https://doi.org/10.48550/arXiv.1412.6980).
- Leite, E. P., and A. C. Vidal, 2011, 3d porosity prediction from seismic inversion and neural networks: Computers & Geosciences, **37**, 1174–1180; doi: [10.1016/j.cageo.2010.08.001](https://doi.org/10.1016/j.cageo.2010.08.001).
- Li, H., Z. Xu, G. Taylor, C. Studer, and T. Goldstein, 2018, Visualizing the loss landscape of neural nets: Advances in neural information processing systems, **31**; doi: [arXiv:1712.09913](https://arxiv.org/abs/1712.09913).
- Lim, J.-S., 2005, Reservoir properties determination using fuzzy logic and neural networks from well data in offshore korea: Journal of Petroleum Science and Engineering, **49**, 182–192; doi: [10.1016/j.petrol.2005.05.005](https://doi.org/10.1016/j.petrol.2005.05.005).

- Ma, Y., S. Cao, J. W. Rector, and Z. Zhang, 2020, Automated arrival-time picking using a pixel-level network: *Geophysics*, **85**, V415–V423; doi: [10.1190/geo2019-0792.1](https://doi.org/10.1190/geo2019-0792.1).
- Mardan, A., and G. Fabien-Ouellet, 2024, Physics-informed attention-based neural networks for full-waveform inversion: 85th EAGE Annual Conference & Exhibition, European Association of Geoscientists & Engineers, 1–5.
- Mardan, A., B. Giroux, and G. Fabien-Ouellet, 2023, Weighted-average time-lapse seismic full-waveform inversion: *Geophysics*, **88**, R25–R38; doi: [10.1190/geo2022-0090.1](https://doi.org/10.1190/geo2022-0090.1).
- Mardan, A., A. Javaherian, and M. Mirzakhani, 2017, Channel characterization using support vector machine: 79th EAGE Conference and Exhibition 2017-Workshops, European Association of Geoscientists & Engineers, cp–519.
- Marsden, D., 1993, Static corrections—a review: *The Leading Edge*, **12**, 115–120; doi: [10.1190/1.1436912](https://doi.org/10.1190/1.1436912).
- McCormack, M. D., D. E. Zauha, and D. W. Dushek, 1993, First-break refraction event picking and seismic data trace editing using neural networks: *Geophysics*, **58**, 67–78; doi: [10.1190/1.1443352](https://doi.org/10.1190/1.1443352).
- Moser, T., 1991, Shortest path calculation of seismic rays: *Geophysics*, **56**, 59–67; doi: [10.1190/1.1442958](https://doi.org/10.1190/1.1442958).
- Murat, M. E., and A. J. Rudman, 1992, Automated first arrival picking: A neural network approach I: *Geophysical prospecting*, **40**, 587–604; doi: [10.1111/j.1365-2478.1992.tb00543.x](https://doi.org/10.1111/j.1365-2478.1992.tb00543.x).
- Nasr, M., B. Giroux, and J. C. Dupuis, 2022, Python package for 3D joint hypocenter-velocity inversion on tetrahedral meshes: Parallel implementation and practical considerations: *Computational Geosciences*, 1–25; doi: [10.1007/s10596-021-10122-6](https://doi.org/10.1007/s10596-021-10122-6).
- Park, M. J., and M. D. Sacchi, 2020, Automatic velocity analysis using convolutional neural network and transfer learning: *Geophysics*, **85**, V33–V43; doi: [10.1190/geo2018-0870.1](https://doi.org/10.1190/geo2018-0870.1).
- Peraldi, R., and A. Clement, 1972, Digital processing of refraction data study of first arrivals: *Geophysical Prospecting*, **20**, 529–548; doi: [10.1111/j.1365-2478.1972.tb00653.x](https://doi.org/10.1111/j.1365-2478.1972.tb00653.x).
- Ronneberger, O., P. Fischer, and T. Brox, 2015, U-Net: Convolutional networks for biomedical image segmentation: *Medical Image Computing and Computer-Assisted Intervention—MICCAI 2015: 18th International Conference, Munich, Germany, October 5-9, 2015, Proceedings, Part III 18*, Springer, 234–241.
- Röth, G., and A. Tarantola, 1994, Neural networks and inversion of seismic data: *Journal of Geophysical Research: Solid Earth*, **99**, 6753–6768; doi: [10.1029/93JB01563](https://doi.org/10.1029/93JB01563).
- Rücker, C., T. Günther, and F. M. Wagner, 2017, pyGIMLi: An open-source library for modelling and inversion in geophysics: *Computers & Geosciences*, **109**, 106–123; doi: [10.1016/j.cageo.2017.07.011](https://doi.org/10.1016/j.cageo.2017.07.011).
- Sabbione, J. I., and D. Velis, 2010, Automatic first-breaks picking: New strategies and algorithms: *Geophysics*, **75**, V67–V76; doi: [10.1190/1.3463703](https://doi.org/10.1190/1.3463703).
- Simon, J., G. Fabien-Ouellet, E. Gloaguen, and I. Khurjekar, 2023, Hierarchical transfer learning for deep learning velocity model building: *Geophysics*, **88**, R79–R93; doi: [10.1190/geo2021-0470.1](https://doi.org/10.1190/geo2021-0470.1).
- Veezhinathan, J., and D. Wagner, 1990, A neural network approach to first break picking: 1990 IJCNN International Joint Conference on Neural Networks, 235–240 vol.1.
- Walia, R., and D. Hannay, 1999, Source and receiver geometry corrections for deep towed multichannel seismic data: *Geophysical research letters*, **26**, 1993–1996; doi: [10.1029/1999GL900402](https://doi.org/10.1029/1999GL900402).
- Wu, H., B. Zhang, F. Li, and N. Liu, 2019, Semiautomatic first-arrival picking of microseismic events by using the pixel-wise convolutional image segmentation method: *Geophysics*, **84**, V143–V155; doi: [10.1190/geo2018-0389.1](https://doi.org/10.1190/geo2018-0389.1).
- Yuan, S., J. Liu, S. Wang, T. Wang, and P. Shi, 2018, Seismic waveform classification and first-break picking using convolution neural networks: *IEEE Geoscience and Remote Sensing Letters*, **15**, 272–276; doi: [10.1109/LGRS.2017.2785834](https://doi.org/10.1109/LGRS.2017.2785834).
- Yuan, S.-Y., Y. Zhao, T. Xie, J. Qi, and S.-X. Wang, 2022, SegNet-based first-break picking via seismic waveform classification directly from shot gathers with sparsely distributed traces: *Petroleum Science*, **19**, 162–179; doi: [10.1016/j.petsci.2021.10.010](https://doi.org/10.1016/j.petsci.2021.10.010).
- Zhao, X., and J. M. Mendel, 1988, Minimum-variance deconvolution using artificial neural networks, *in* SEG Technical Program Expanded Abstracts 1988: Society of Exploration Geophysicists, 738–741.
- Zhu, W., and G. C. Beroza, 2019, PhaseNet: A deep-neural-network-based seismic arrival-time picking method: *Geophysical Journal International*, **216**, 261–273; doi: [10.1093/gji/ggy423](https://doi.org/10.1093/gji/ggy423).
- Zwartjes, P., and J. Yoo, 2022, First break picking with deep learning—evaluation of network architectures: *Geophysical Prospecting*, **70**, 318–342; doi: [10.1111/1365-2478.13162](https://doi.org/10.1111/1365-2478.13162).